SMALL LEADING-EDGE FLAP FOR POST-STALL FLOW CONTROL ON A 45-DEG DELTA WING

Takashi Matsuno, Shigeru Yokouchi, Yoshiaki Nakamura
Department of Aerospace Engineering, Nagoya University
464-8603 Nagoya, JAPAN

Keywords: *High angle-of-attack aerodynamics, Delta wing, Flow control device*

Abstract

The characteristics of rolling moment in a 45-deg delta wing with a leading-edge flap were studied to examine its effects in pre- and post-stall high angle-of-attack regimes, where conventional control surfaces are ineffective. A small flap was employed to control the flow, which was placed on the round leading-edge of the delta wing from 10% to 75% chord with a height of 2 mm. The wind-tunnel experiments were carried out for static aerodynamic force measurements and flow visualization. In the pre-stall moderate angle-of-attack regime, it is observed that the single flap can produce about ± 0.01 of rolling moment coefficient, which is sufficient for flight control. On the other hand, in the post-stall high angle-of-attack regime, its rolling moment characteristics are quite nonlinear and complex. The flap can basically reduce the unsteady moment by interfering with the development of an leading-edge vortex, or promoting the flow attachment to the wing surface.

1 Introduction

In modern high agility aircraft, asymmetry of leading-edge vortices can cause unwanted motions at high angles of attack. Wing rock, a self-induced oscillation in roll, is one of these motions. Since it can cause severe safety problems, this phenomenon has been studied by many researchers [1, 2, 3, 4]. Recently, we found that a self-induced roll oscillation also occurs on a 45° sweep delta wing with round leading-edges [5, 6, 7].

In such situation, conventional control surfaces are ineffective, because unsteady separated flow on the surface reduces their effects. Especially, in roll maneuver, an effective and efficient control method is needed both for providing high agility in turning flight and for suppressing unwanted motions. In recent years, due to the improvement of microelectronics, some researchers choose very small devices, such as micro electromechanical systems (MEMS), as an actuator to flow control [8].

The objective of the present study is to control the flow around a delta wing by using a small device. More specifically, the small leading-edge flaps are selected to control leading-edge vortices. To understand the basic characteristics of the flap effects, static aerodynamic force measurements and flow visualization have been carried out in cases with and without the small flaps. Based on these results, the effects of the flaps on aerodynamics in a high-alpha regime will be discussed.

2 Concept of Control Device

In this study, a small flap was selected to control the flow. The flap was placed on the leading-edge of the delta wing from 10% to 75% chord with a height of 2 mm, as shown in Fig. 1.

At an AOA less than the stall angle, the flap is designed to control the location of the leading-edge vortex by varying flap angle, following the

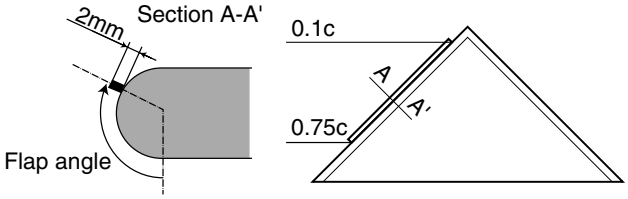

Fig. 1 Geometries of small flap and definition of flap angle.

idea of Ho et al[8]. For post-stall flight, two additional effects are expected. One is that the separation line is fixed on the leading-edge, which reduces the unfavorable effects exerted by unsteadiness of the separated flows. The other effect is that flow reattachment may occur at some roll angle. This would stabilize the wing and prevent wing drop which occurs by a partial stall of wing.

The effects of flap angle on rolling moment are focused in this paper. The location of the flap is defined as the angle θ from the bottom surface, as shown in Fig. 1.

3 Experimental Set-Up

All experiments were conducted by the closed-return low speed wind tunnel at the Department of Aerospace Engineering, Nagoya University. The tunnel has an open test section of 900mm wide × 750mm high. In this study a 45-deg delta wing model with round leading-edges was employed (Fig. 2). Specifications of the model are indicated in Table 1.

Aerodynamic force measurements were carried out by using a six-components strain-gauge sting balance. The schematic of the present experiments is shown in Fig. 3. The force balance data were collected by using a dynamic strain amplifier with a Wheatstone bridge, and stored in a PC through a DAQ board. Since the 6-component force balance was set at some distance from the center of gravity of the model, measured forces were converted to the data around the center of gravity of the model by calculation.

Surface flow was visualized with an oil-flow method. The oil used here is a mixture of titanium dioxide, oleic acid and dimethyl silicone fluid with very low viscosity. In the experiment, the oil was spread on the wing model that was fixed an angle of attack and a roll angle, and evaporated by the uniform flow, showing clear skin friction lines. The visualized skin-friction lines were photographed by a digital still camera, and post-processed with a PC. Motions of the oil were also taken with a digital video camera, as a supplement to interpret the flow patterns.

All the experiments were conducted with a freestream velocity of 20 m/s and a Reynolds number of 220,000, based on the root chord.

Table 1 Specifications of wing model.

Parameter	Specifications
Sweep Angle [deg]	45°
Root Chord c_r [mm]	160
Span b [mm]	320
Wing Area S [m^2]	2.56×10^{-2}
Aspect Ratio	4.0
Thickness Ratio, t/c_r	9.1%
Inertial Moment [kgm^2]	5.40×10^{-4}
Leading Edge Profile	Half Circle
Material	FRP / composite

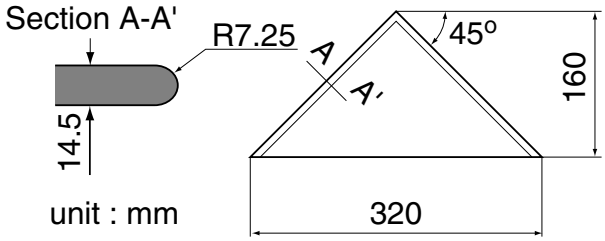

Fig. 2 Dimensions of wing model.

4 Results and Discussion

4.1 Characteristics in a pre-stall regime

First, the effects of the flap on roll characteristics in a pre-stall regime is presented. In this regime the aerodynamic characteristics are rather linear compared with those in a post-stall regime. Therefore we focused on the case of roll angle $\phi = 0°$, assuming that a displacement in roll angle would not cause a remarkable change in the

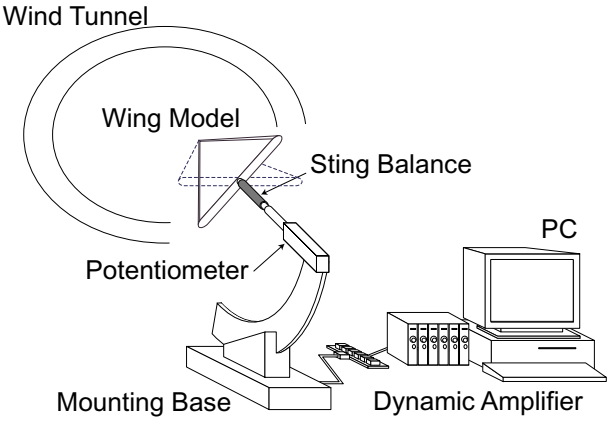

Fig. 3 Schematic of wind-tunnel experiment.

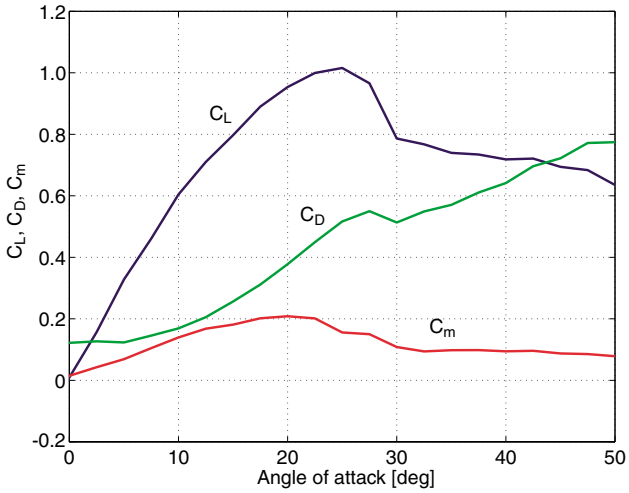

Fig. 4 Longitudinal aerodynamic characteristics.

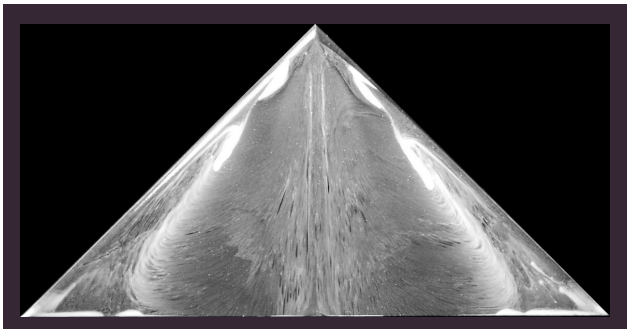

Fig. 5 Surface skin-friction lines at $\sigma = 20°$.

aerodynamic characteristics. The effects will be examined, regarding changes in rolling moment and flow pattern from the baseline case without the flap. From these observations, the concept of the present smail flap will be validated, and the main source to those effects will be sought.

4.1.1 Basic characteristics/flow field

Before discussing the effects of the flap, we will describe the longitudinal aerodynamic characteristics of the wing model and flow patterns at pitch angle $\sigma = 20°$. Figure 4 shows C_L, C_D, and C_m versus angle of attack. The lift coefficient takes its maximum value at $\alpha \simeq 25°$, and the wing loses lift and stalls beyond this angle.

At $\sigma = 20°$, near or beyond the stall angle, leading-edge (LE) vortices burst over the top surface and lift off at $x/c \simeq 0.4$ as shown in Fig. 5. Since the vortex breakdown reduce the vortex lift component, an increment in the lift in this pitch angle region mainly comes from the potential-flow component in the bottom wing surface. Therefore, in this region, the best way to extend the $C_{L_{max}}$ is to delay the LE vortex breakdown. Also, this approach could enables a roll control of the wing, by vary the breakdown location with each wing half on purpose, at the same time.

4.1.2 Rolling moment

Figure 6 presents changes in the rolling moment due to flap location at $\sigma = 20°$. ΔC_l is defined as $\Delta C_l = C_l(\text{flap-on}) - C_l(\text{flap-off})$. Although the phenomenon is quite nonlinear, the flap could generate both positive and negative rolling moments; that is, flap-installed wing half moves up and down, depending on flap angle. Specifically, two peaks of rolling moment are significant at flap angle $\theta = 90°$ and $150°$. In the region of θ less than $\theta = 90°$ peak, ΔC_l is rather nonlinear, and the value of which is varied in each run. In contrast, from $\theta = 90°$ to $150°$, its characteristics are linear and show good repeatability, implying that the flow pattern is rather steady. At these two peaks, some changes in flow field should occur, which will be discussed later.

These results show the efficiency of this kind LE flap as flow-control device. The flap could take the rolling moment coefficient of about 0.01, at $\sigma = 20°$, which is enough for flight control.

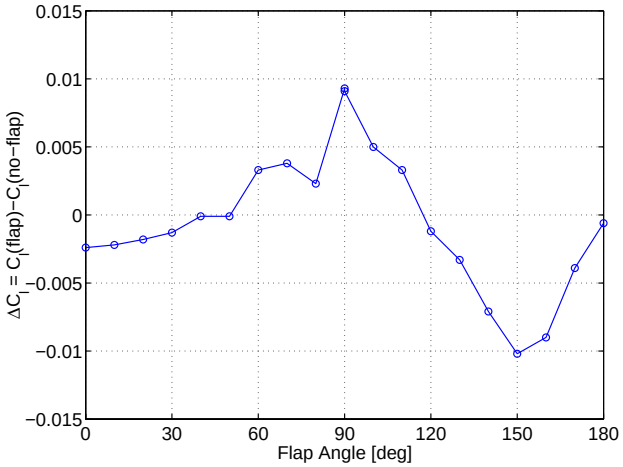

Fig. 6 Effect of flap location on rolling moment difference.

4.1.3 Flow field and mechanism

Figure 7 shows some data obtained by the oil-flow visualization at $\sigma = 20^\circ$ for the case with the flap. As for the flow field, there are three regimes of flow patterns as a function of flap angle. At the boundaries of these flow regimes, changes occur on the flow topology. It is not only on a location of separation or breakdown bubble, but the structure of the flow field changes suddenly. They correspond to regimes in the characteristics of rolling moment shown in Fig. 6: (i) $\theta < 50^\circ$, (ii) $50^\circ < \theta < 90^\circ$, (iii) $90^\circ < \theta < 150^\circ$, and (iv) $150^\circ < \theta$.

(i) $\theta < 50^\circ$ When flap angle is less than 50 deg, the increment of rolling moment ΔC_l is relatively small. In this case, the flow field on the top surface shows no significant change, as shown in Fig. 7(a). The flow field is basically symmetric between port and starboard, although some difference can be observed in locations of focus and a primary LE vortex. Another experiments have clarified that the primary attachment line lies on about $\theta = 50^\circ$ for the plain delta wing. This supports the argument that the flow on the top surface is not affected by the flap installed at $\theta < 50^\circ$. Thus, the negative value of $DeltaC_l$ in this regime is due to a contribution of bottom surface, for example, a small vortex that forms at a bottom surface of the flap.

(ii) $50^\circ < \theta < 90^\circ$ Setting flap angle larger than 50 deg, the flow field on the flap side undergoes a significant change. As Fig. 7(b) shows, the baseline flow structure seen at $\theta = 50^\circ$ was broken on the flap side, and an isolated flow region appears (see Fig. 8). This region seems to be isolated with a shear layer from the LE flap, and inside the region there is a flap LE vortex which originates from the forward end of the flap. The region is formed by the interaction between a separated flow and the flap vortex. By this complex interaction, the shear layer, which forms the primary LE vartex, is pulled toward the leading edge, and the attached flow region is enlarged. As a result, the local lift increases on the flap-side, so that the wing gains positive(flap-side up) rolling moment increment. This occurs, because the flap is located very close to the primary attachment line and it breaks the flow structure around the leading edge for the baseline.

(iii) $90^\circ < \theta < 150^\circ$ A swirling flow is predominant on the wing surface in this regime, as shown in Fig. 7(c). This indicates that the LE vortex on the flap side lifts off from the wing surface by the flap. This evidently reduces the vortex load, resulting in negative rolling moment increment. The amount of ΔC_l depends on the displacement length of the LE vortex from the surface; thus the ΔC_l decreases with flap angle.

(iv) $150^\circ < \theta$ In this regime, the effect of the flap gradually decreases, because the flap location becomes far away from the primary attachment line. On the other hand, the flap angle still affects the height of the LE vortex. At the $\theta = 150^\circ$ peak, these two factors are balanced, so that $\partial(\Delta C_l)/\partial\theta$ becomes zero.

From these results, it is confirmed that the flap can sufficiently work as a roll control device at a moderate AOA. However, the mechanism by which the flap works is different from the primary concept, that follows the idea of Ho et al[8]. It seems that this comes from the difference in sweptback angle. The 45deg-swept delta wing employed here produces relatively weak LE

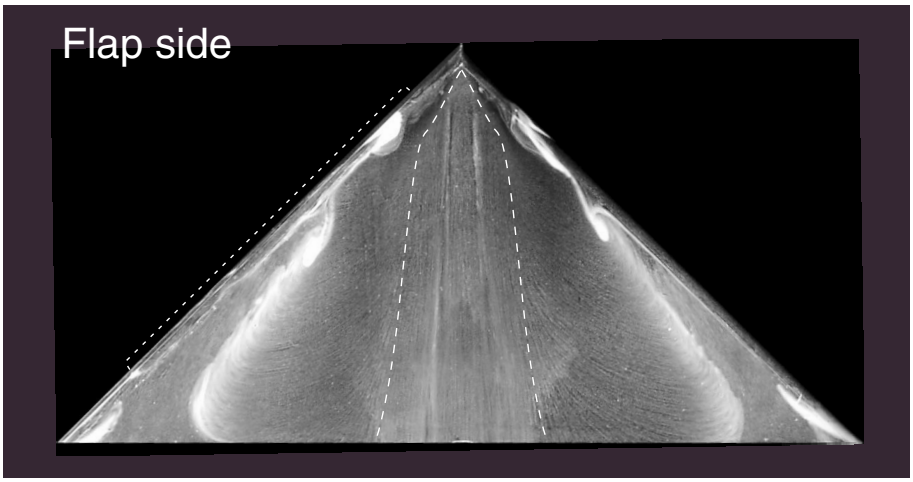

a) θ **= 50deg.**

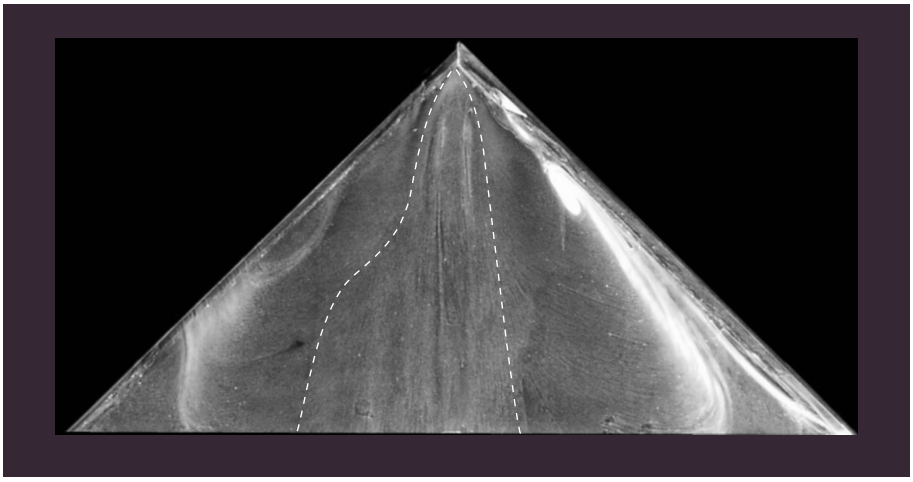

b) θ **= 80deg.**

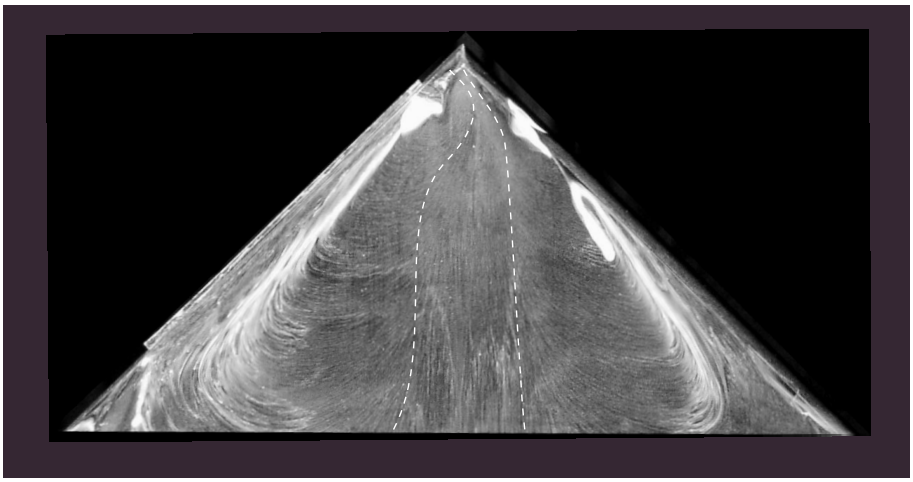

c) θ **= 120deg.**

Fig. 7 Oil-flow patterns at $\sigma = 20^\circ$ **with a flap.**

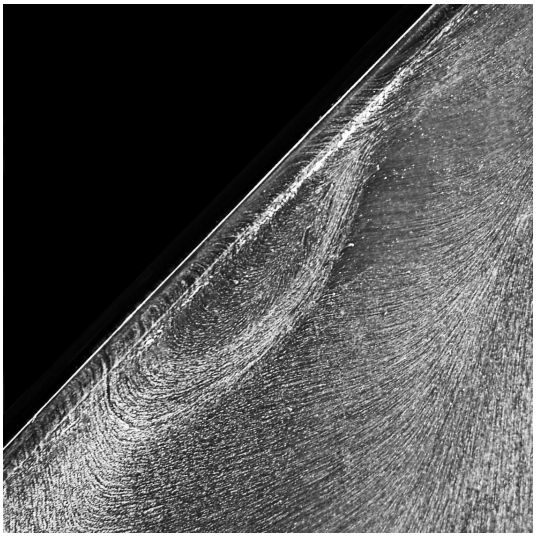

a) Oil-flow pattern.

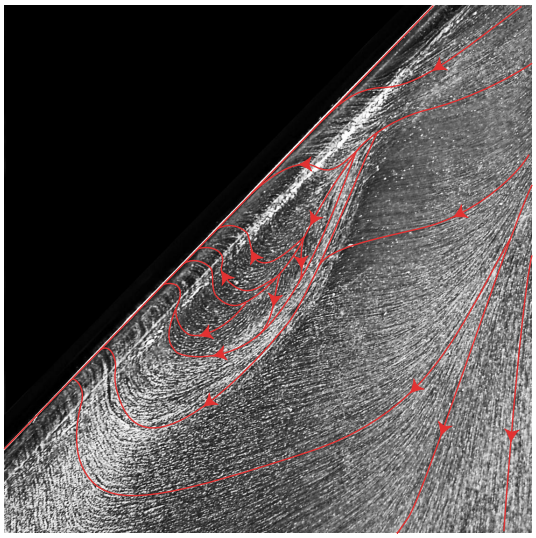

b) Interpretation of skin-friction lines.

Fig. 8 Close-up of an interacting region on flap side.

vortices that will be easily broken by small disturbances.

4.2 Characteristics in post-stall regime

4.2.1 Basic characteristics and flow field

Figure 9 shows characteristics of the static rolling moment for the plain delta wing at $\sigma = 30^\circ$, where the wing stalls and no vortex lift component is produced[6].

The characteristics of the rolling moment are discontinuous and nonlinear, with three roll attractors at roll angle $\phi = 0^\circ$ and $\phi = \pm 55^\circ$. In $|\phi| < 15^\circ$ the wing is linearly stable about $\phi = 0^\circ$. In the regions around $\phi = \pm 55^\circ$, the wing is statically stable with nonlinear characteristics, which is different from the region in $|\phi| < 15^\circ$. At $|\phi| = 15^\circ$, there are discontinuous changes in the sign of C_l, one of which is denoted as A in Fig. 9. This means that the direction of the attracting force changes, whether the wing is in $|\phi| < 15^\circ$ or $|\phi| > 15^\circ$.

Furthermore, there are various critical states, in which the aerodynamic characteristics change discontinuously. In $15^\circ < |\phi| < 55^\circ$, where the wing is attracted to a deeper roll angle, there also exist some critical states in small roll-angle regions (B and C in Fig. 9).

The wing model performs self-induced roll oscillations in such regimes[6]. The motions do not show a single limit cycle, but fluctuate in a region consisting of "limit cycles" without converging to a single trajectory. These self-induced oscillations have different characteristics from a slender wing rock with a precise single limit cycle, and there are complicated unsteady behaviors of rolling moment in each cycle.

Regarding the flow pattern, at this pitch angle the flow completely separates from the wing surface, and does not form any vortex that can produce vortex lift, as shown in Fig. 10. As ϕ increases, the flow changes discontinuously. At a certain roll angle, some vortices are formed on the leeward wing half. When roll angle increases further, the flow changes unsteadily between a full separation and an attached flow in the windward wing half, through a transitional state with

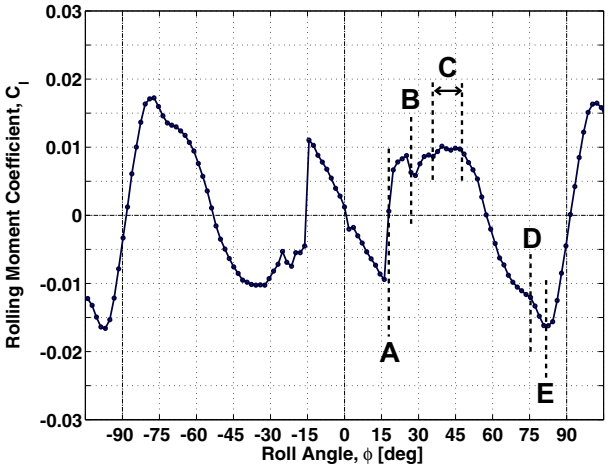

Fig. 9 Rolling moment characteristics at $\sigma = 30°$.

vortex cores.

Figure 11 shows an example of the surface skin-friction lines for the case with $\sigma = 30°$ and $\phi = 50°$. In such a deep roll-angle regime, the flow field over the wing seems to be quite complex. Due to asymmetrical change in effective sweep angle between the port and starboard wing halves, the flow field on the leeward side becomes similar to that on a slender wing. On the other hand, the flow field on the windward side becomes similar to that on a straight wing. In actual flow field, these two flow patterns interact each other, so that a complex flow field is formed, as shown in Fig. 11(b). Especially at the windward wing half (starboard in this figure), the flow field is affected by the LE vortex on the leeward and a reversed flow from the trailing edge as well as a separated flow from the windward leading edge. The schematic of the supposed flow field is presented in Fig. 11(c).

Figure 12 shows overall characteristics regarding change in flow pattern due to roll angle. To reduce unwanted roll motions, the present aerodynamic device is expected to work well in such flow behaviors in the post-stall regime.

4.2.2 Rolling moment

Figure 13 presents the characteristics on rolling moment coefficient concerning the wing with the flap at $\sigma = 30°$. In this study the flap was pri-

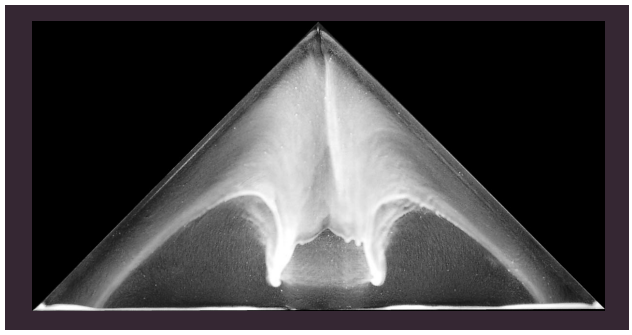

Fig. 10 Surface skin-friction lines at $\sigma = 30°$.

marily mounted on a port wing half, as shown in Fig. 1. However in this case, characteristics at a post-stall regime, the flap was set at port or starboard wing half in each experiment to see the effects of the flap for each side. In Fig. 13(a) the flap was mounted on the port, while in Fig. 13(b) it on the starboard. Since the experiments were carried out for positive roll angles only, the flap on the port side corresponds to the leeward, while that on the starboard to the windward.

In the leeward case shown in Fig. 13(a), the effect of the flap is mainly seen in $15° < \phi < 55°$. There, the flap can basically reduce the unsteady moment, which is well represented by the formation of an LE vortex on the leeward (see Fig. 12). The effect becomes significant when $\theta > 80°$. The flap affects the LE vortex on the leeward, such a way that it comes to interfere with the formation of the LE vortex with increasing roll angle. This occurs because the flap makes the leading-edge shape sharp; thus the breakdown location of LE vortex gradually moves toward the trailing edge, so that development of the unstable rolling moment is delayed. As a result, at $\theta = 150°$, the unstable rolling moment vanishes, and the wing trims only at $\phi = 0°$. This suppress the self-induced oscillations of non-slnder delta wings[6, 9].

In the windward-flap case, the characteristics become quite different and difficult to interpret the whole flow mechanism in a straitforward way, because the flap on this side affects on the complicated and full-separated flow described above. Many significant effects seem to be included in Fig. 13(b), where the most drastic changes are

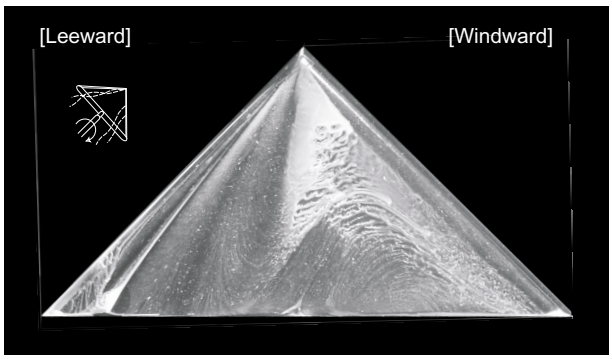

a) Surface skin-friction lines.

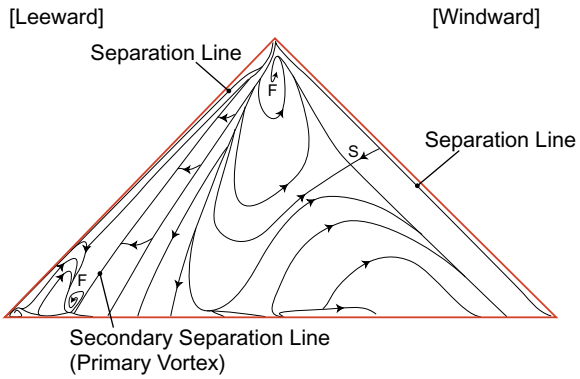

b) Interpretation of surface flow topology.

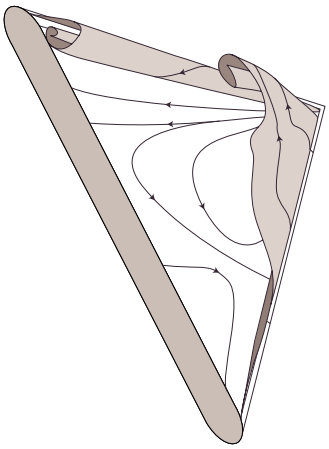

c) Schematic of the flow field.

Fig. 11 Flow field at $\sigma = 30^\circ$ and $\phi = 50^\circ$.

observed at $\phi = 45^\circ \sim 75^\circ$ for $\theta = 100^\circ$. The roll undamping is decreased; that is, the local lift is recovered on the windward wing half. Figure 14 shows the change in flow field in this case. The flap at $\theta = 100^\circ$ can promote the flow attachment to the wing surface by changing the relative angle of incidence.

In the post-stall regime, the effect of flap is quite nonlinear and complex, as in the baseline delta wing. However, the results obtained in the present experiments show that the flap could vary the rolling moment sufficiently to control an attitude of wing. Thus, even though it might be difficult to control the whole flow field as we like, small devices such as the present flap turned to be effective in roll control. As for application to complicated configuration such as actual aircraft, further study is necessary.

5 Conclusion

The characteristics of rolling moment in a 45-deg delta wing were examined, and the effects of a leading-edge flap were studied.

In a pre-stall moderate angle-of-attack regime, the flap produces rolling moment, which is enough for flight control. The flap generated both directions of rolling moment, that is flap-side up and down, depending on the flap installment angle. From the results obtained here, the present flow-control device was confirmed to be effective.

In a post-stall high angle-of-attack regime, the rolling moment characteristics with the flap became quite nonlinear and complex, as in the baseline delta wing. When the flap was set on the leeward wing half, the flap can basically reduce the unsteadiness of rolling moment by interfering with the formation of an LE vortex with increasing roll angle. At $\theta = 150^\circ$, the unstable rolling moment vanishes. On the other hand, in the windward-flap case, the characteristics became quite different from the leeward-flap case, because the flap affects the complicated and full-separated flow. At some flap angles in the windward case, the flap can promote the flow attach-

ment to the wing surface, resulting in a decrease of roll undamping.

Although the flap has nonlinear characteristics, the results obtained in the present experiments show that the small flap could control the rolling moment sufficiently.

6 Acknowledgments

This research was supported by the Japan Society for the Promotion of Science. This support is gratefully acknowledged. We also wish to acknowledge the kindness of Mitsubishi Heavy Industries, Ltd. for allowing us to use an accurate 6-component force balance.

References

[1] Levin D and Katz J. Dynamic load measurements with delta wings undergoing self-induced roll oscillation. *Journal of Aircraft*, Vol. 21, No 1, pp 30–36, 1984.

[2] Ng T. T, Malcolm G. N, and Lewis L. C. Experimental study of vortex flow over delta wing in wingrock motion. *Journal of Aircraft*, Vol. 29, No 4, pp 598–603, 1992.

[3] Ericsson L. E. The fluid mechanics of slender wing rock. *Journal of Aircraft*, Vol. 21, No 5, pp 322–328, 1984.

[4] Jenkins J. E, Myatt J. H, and Hanff E. S. Body-axis rolling motion critical states of a 65-degree delta wing. *Journal of Aircraft*, Vol. 33, No 2, pp 268–278, 1996.

[5] Ueno M, Matsuno T, and Nakamura Y. Unsteady aerodynamics of rolling delta wings with high aspect ratio. AIAA Paper 98–2520, 1998. In 16th AIAA Applied Aerodynamics Conference Proceedings.

[6] Matsuno T and Nakamura Y. Self-induced roll oscillation of 45-degree delta wings. AIAA Paper 2000–0655, 2000.

[7] Ericsson L. E. Wing rock of non-slender delta wings. AIAA Paper 2000–0137, 2000.

[8] Tai Y.-C and Ho C. Mems devices for flow control. AIAA Paper 97–1787, 1997.

[9] Matsuno T, Yokouchi S, and Nakamura Y. The effect of leading-edge profile on self-induced oscillation of 45-degree delta wings. AIAA Paper 2000–4004, 2000.

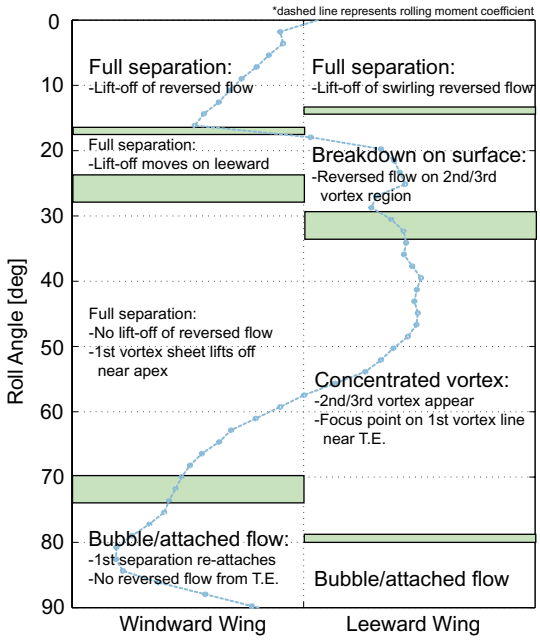

Fig. 12 Skin-friction topology change for $\sigma = 30°$.

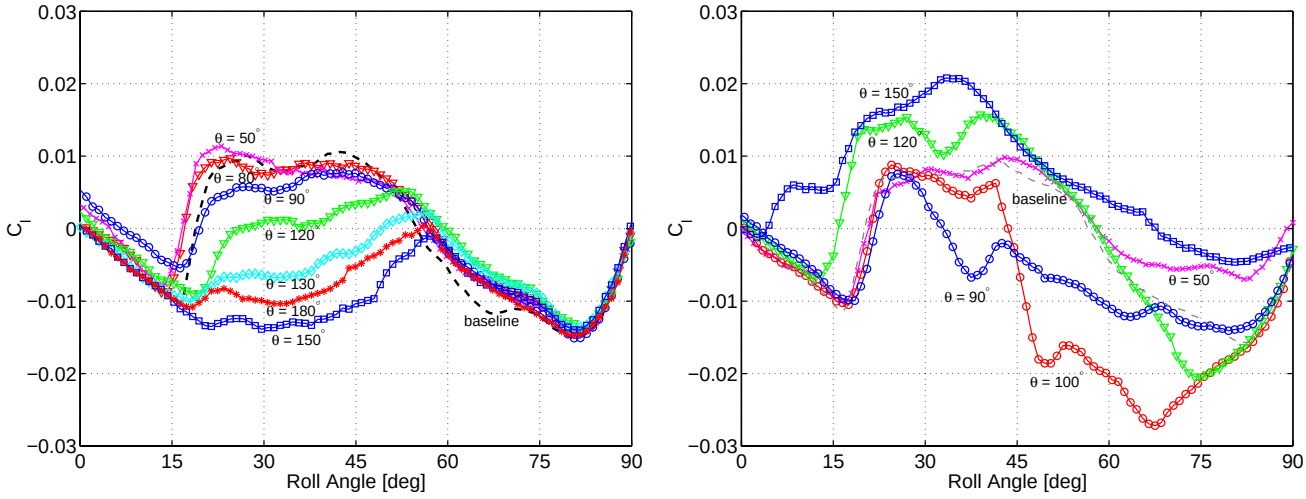

a) Flap on the leeward side. **b) Flap on the windward side.**

Fig. 13 Rolling moment difference vs roll angle with flap angle as parameter.

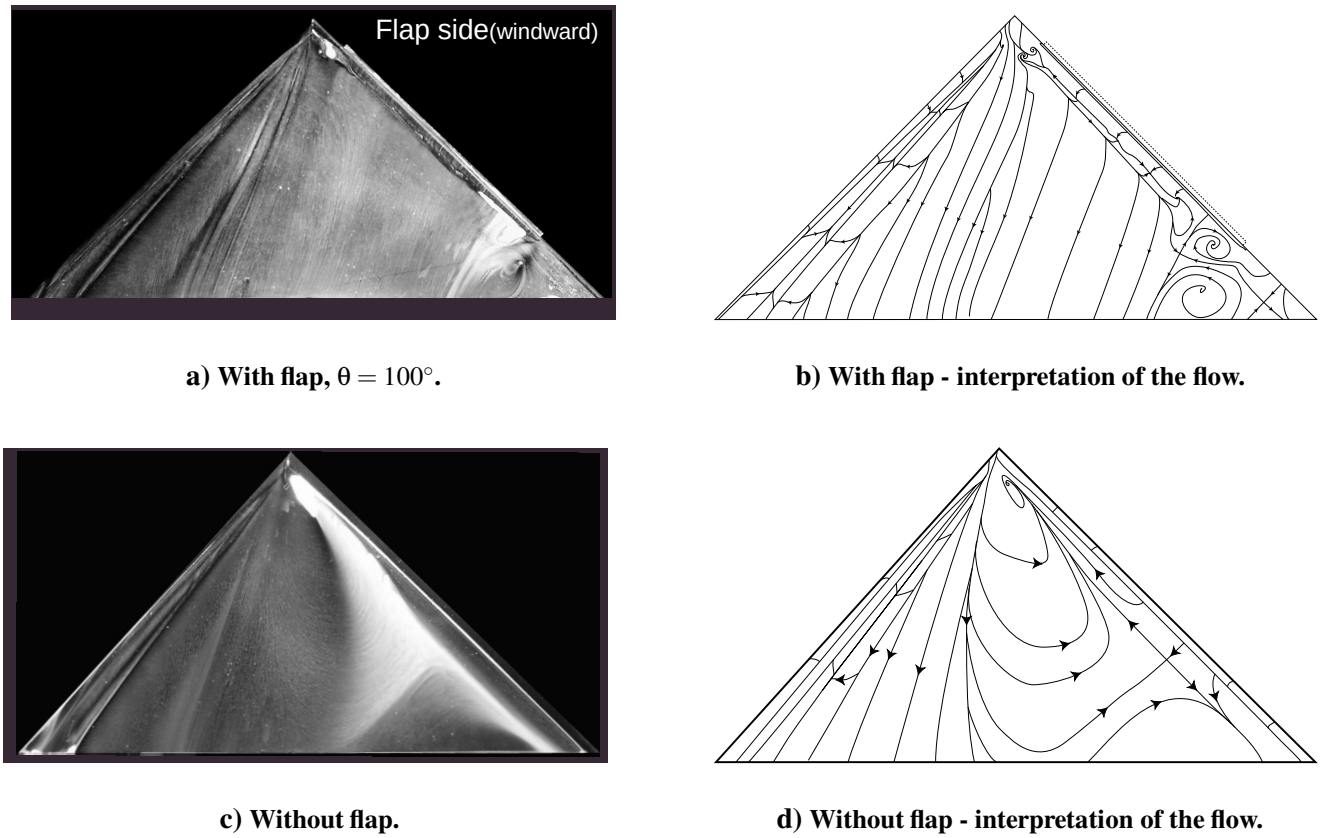

a) With flap, $\theta = 100°$. **b) With flap - interpretation of the flow.**

c) Without flap. **d) Without flap - interpretation of the flow.**

Fig. 14 Flow patterns at $\sigma = 30°$ and $\phi = 65°$ with flap.